

## **TEACHING-LEARNING-BASED PARAMETRIC OPTIMIZATION OF AN ELECTRICAL DISCHARGE MACHINING PROCESS**

**Vidyapati Kumar<sup>1</sup>, Sunny Diyaley<sup>2</sup>, Shankar Chakraborty<sup>3</sup>**

<sup>1</sup>Central Institute of Mining and Fuel Research, Dhanbad, Jharkhand, India

<sup>2</sup>Department of Mechanical Engineering, Sikkim Manipal Institute of Technology,  
Sikkim Manipal University, Majitar, Sikkim, India

<sup>3</sup>Department of Production Engineering, Jadavpur University, Kolkata, West Bengal, India

**Abstract.** *Due to several unique features, electrical discharge machining (EDM) has proved itself as one of the efficient non-traditional machining processes for generating intricate shape geometries on various advanced engineering materials in order to fulfill the requirement of the present day manufacturing industries. In this paper, the machining capability of an EDM process is studied during standard hole making operation on pearlitic SG iron 450/12 grade material, while considering gap voltage, peak current, cycle time and tool rotation as input parameters. On the other hand, material removal rate, surface roughness, tool wear rate, overcut and circularity error are treated as responses. Based on single- and multi-objective optimization models, this process is optimized using the teaching-learning-based optimization (TLBO) algorithm, and its performance is contrasted against firefly algorithm, differential evolution algorithm and cuckoo search algorithm. It is revealed that the TLBO algorithm supersedes the others with respect to accuracy and consistency of the derived optimal solutions, and computational efforts.*

**Key Words:** *EDM Process, TLBO Algorithm, Metaheuristics, Optimization*

### 1. INTRODUCTION

Electrical discharge machining (EDM) has already been accepted as an efficient thermo-electrical material removal process in tool and die making, aerospace and automotive industries, and also in finishing of surgical components due to its ability to maintain close tolerances and attain higher dimensional accuracy [1, 2]. In this process, a series of successive discharges between the tool (electrode) and the workpiece is responsible

---

Received February 18, 2020 / Accepted June 08, 2020

**Corresponding author:** Shankar Chakraborty

Department of Production Engineering, Jadavpur University, Kolkata, West Bengal, India

E-mail: s\_chakraborty00@yahoo.co.in

for removing material in the presence of a dielectric medium (kerosene or de-ionized water). During electrical discharge, a discharge channel is developed having a temperature around 12000°C causing melting and evaporation of material from the workpiece surface. The electrode is advanced towards the workpiece until the inter-electrode gap is small enough for the higher impressed voltage to ionize the dielectric [3]. In EDM process, a perfect replication of the tool shape is generated on the workpiece surface. This process is especially suitable for generating complex shape profiles on electrically conductive materials with low machinability [4].

As there is no direct contact between the tool and the workpiece, this process is free from any mechanical stress generation, chatter/burr formation and vibration problem. Its machining performance is also uninfluenced by the hardness of the work material because the material removal takes place by melting due to high intensity localized heat generation. Since no cutting force is generated, extremely deep narrow holes with high aspect ratio can be machined using this process with minimum tool wear. It can even generate intricate cavities in a single operation. But EDM process also suffers from several drawbacks, like generation of recast layer and heat-affected zone (HAZ), low material removal rate (MRR), high machining time and related cost, low flexibility, capability of machining only electrically conductive materials, etc.

It has been observed that the machining performance of an EDM process with respect to MRR, surface roughness (SR), tool wear rate (TWR), HAZ, radial overcut (ROC) etc. is significantly affected by different electrical parameters (peak current, pulse-on time, pulse-off time, gap voltage, polarity, etc.) and non-electrical parameters (electrode material, type of the dielectric used, dielectric pressure, rotation of the electrode, etc.). Thus, in order to fulfill the requirements of better response values, it is always preferred to operate an EDM set-up while maintaining the settings of its different input parameters as their optimal levels. It would also lead to a higher production rate with reduced machining time.

Keeping in mind the requirements of finding out the optimal parametric mixes for EDM processes, this paper deals with the application of teaching-learning-based optimization (TLBO) algorithm to study the influences of various input parameters of an EDM process on its responses (outputs) while machining pearlitic SG iron 450/12 grade work material. For this process, gap voltage, peak current, cycle time and rotation of the tool are considered as input parameters, whereas, MRR, SR, TWR, overcut (OC) and circularity error (CE) are treated as responses. Both the single- and multi-objective optimization models are developed and subsequently solved using the considered algorithm. Its optimization performance is also contrasted with that of firefly algorithm (FA), differential evolution (DE) algorithm and cuckoo search (CS) algorithm. The TLBO algorithm supersedes the other algorithms with respect to accuracy and consistency of the derived optimal solutions, and computational effort. The results of two-tailed paired *t*-tests also confirm its superiority over the others.

## 2. REVIEW OF THE LITERATURE

Mandal et al. [5] first applied artificial neural network (ANN) with back-propagation algorithm to model an EDM process and non-dominating sorting genetic algorithm-II (NSGA-II) was later adopted to optimize the said process. Using controlled elitist NSGA technique, Bharti et al. [6] optimized different input parameters of a die-sinking EDM process. The ANN with back-propagation algorithm was also adopted to model the

considered process. Baraskar et al. [7] employed NSGA-II technique to identify the optimal settings of pulse-on time, pulse-off time and discharge current for an EDM process to achieve better values of SR and MRR responses. Shivakoti et al. [8] studied the effects of salt-mixed de-ionized water as a dielectric on MRR, TWR, ROC and taper during EDM operation of D3 die steel. The Taguchi method was later utilized to optimize the considered EDM process parameters. Aich and Banerjee [9] applied weight-varying multi-objective simulated annealing technique to develop the corresponding Pareto optimal front for simultaneous optimization of MRR and SR in an EDM process. Radhika et al. [10] considered peak current, pulse-on time and flushing pressure as the input parameters of an EDM process. A hybrid optimization technique consisting of ANN and genetic algorithm (GA) was later employed to minimize SR and TWR, and maximize MRR. A Pareto-optimal front was also developed offering a set of non-dominated solutions. Tiwari et al. [11] applied GA technique to simultaneously optimize MRR and SR during an EDM operation. The corresponding Pareto-optimal solutions were subsequently proposed. Mazarbhuiya et al. [12] performed eight experimental runs in an EDM set-up based on Taguchi's design plan, and applied grey relational analysis (GRA) technique to determine the optimal settings of discharge current, flushing pressure, pulse-on time and polarity for achieving maximum value of MRR and minimum SR value. Mohanty et al. [13] considered open circuit voltage, discharge current, pulse-on time, duty factor, flushing pressure and type of the tool material as the control parameters of a die-sinking EDM process. Based on a multi-objective particle swarm optimization (PSO) algorithm, the optimal values of different process responses, like MRR, EWR, SR and ROC were subsequently determined. While considering peak current, polarity, pulse-on time, gap voltage and spindle speed as the input parameters of an EDM process, Gohil and Puri [14] adopted Taguchi-GRA technique to maximize MRR and minimize SR while machining titanium alloys. Satpathy et al. [15] combined principal component analysis with technique for order of preference by similarity to ideal solution (TOPSIS) for multi-objective optimization of an EDM process, while taking into account peak current, pulse-on time, duty cycle and gap voltage as the input parameters, and MRR, TWR, ROC and SR as the responses. Applying VIKOR index as a multi-objective optimization tool for an EDM process, Mohanty et al. [16] determined the optimal settings of current, pulse-on time and voltage for having better values of MRR, TWR, SR and ROC. Singh et al. [17] utilized NSGA-II technique to optimize MRR and TWR in an EDM process while considering peak current, pulse-on time, pulses-off time and gap voltage as the input parameters. Gostimirovic et al. [18] modeled the energy efficiency of an EDM process with respect to MRR and SR responses. Evolutionary multi-objective optimization was later performed to derive a set of optimal solutions for discharge energy taking into account discharge current and discharge duration as the input parameters. Ramprabhu et al. [19] applied passing vehicle search (PVS) as a multi-objective optimization tool for optimizing various input parameters of an EDM process. The performance of the adopted technique was also compared with that of other intelligent computing models. Based on GRA technique, Tharian et al. [20] performed multi-objective optimization of MRR and SR during EDM operation of Al7075 alloy. Huu et al. [21] proposed the application of multi-objective optimization based on ratio analysis (MOORA) method for having better values of MRR, SR and TWR during EDM operation of SKD61 die steel with low-frequency vibration. Analytic hierarchy process (AHP) was utilized to estimate relative weights of the considered responses. While employing response surface methodology (RSM)-based regression models, Niamat et al. [22] endeavored to study the

influences of current, pulse-on time and pulse-off time on MRR, SR and TWR in an EDM process. Multi-objective optimization was also performed to achieve sustainability while optimizing the conflicting responses.

The above-cited review of the existing literature reveals that parametric optimization of EDM processes has already caught the attention of the research community, and several optimization techniques, like GA, NSGA-II, simulated annealing, PVS, PSO, etc. have been applied in this direction. Those adopted algorithms have too many algorithmic parameters, which if not properly tuned, may increase the computational effort and result in local optimal solutions. Similarly, numerous multi-criteria decision making approaches, such as VIKOR, TOPSIS, GRA, AHP, MOORA, etc. have also been utilized to determine the most feasible parametric mixes for EDM processes. But, in most of the cases, near optimal or sub-optimal solutions have been arrived at. Moreover, there is a scarcity of research works dealing with comparative analysis of the optimization performance of the available metaheuristic algorithms. In order to overcome such drawbacks, the TLBO algorithm is applied in this paper for the first time to find out the best combination of four EDM process parameters while machining pearlitic SG iron 450/12 grade work material in order to simultaneously optimize the responses under consideration. The TLBO algorithm is a population-based optimization technique, requiring no algorithmic specific parameters and has already earned a broad acceptance among the researchers in the optimization domain. This algorithm is efficient, simple and capable of achieving almost global optimal solutions with less computational effort. The comparative analysis results reveal that it is more flexible, robust and reliable as compared to other mostly preferred metaheuristic algorithms, like FA, DE and CS techniques. Their optimization performance is compared with respect to three metrics, i.e. accuracy of the derived solutions, consistency of the solutions and convergence speed. These comparison results are also validated using the developed boxplots and paired *t*-test.

### 3. TLBO ALGORITHM

The TLBO algorithm is based on the concept of improving knowledge of the students within the classroom by the teacher first, and the knowledge is further upgraded by the mutual interaction among the students [23]. This algorithm thus consists of two phases, i.e. a) teacher phase and b) student phase. The knowledge acquired by the students from the teacher is known as the teacher's phase. On the other hand, enrichment in knowledge through mutual interactions among the students is known as the student's phase [24].

#### *Teacher Phase*

In this algorithm, the teacher is supposed to be the best solution in an entire set of solutions and the learners acquire knowledge from the teacher. A teacher always attempts to improve the grades of all the students in the class by bettering the mean result of the entire class. But, from the practical point of view, it is not at all possible to uplift the mean result of the class because the learning capability of the class depends on the ability of the students to grab knowledge from the concerned teacher. Let  $X_{j,k,i}$  be any value in the solution, where  $j$  is the design variable (subject taken by the learners) ( $j = 1, 2, \dots, m$ );  $k$  is the population member (i.e. learner) ( $k = 1, 2, \dots, n$ ) and  $i$  is the iteration number ( $i = 1, 2, \dots, Gen_{max}$ ) ( $Gen_{max}$  is the number of maximum iterations). The teacher phase begins

with the identification of the teacher (best solution) from the available population, based on the objective function value. At  $i^{\text{th}}$  iteration,  $X_{k,i}$  represents the best solution having the value of  $f(X_{k,i})$  being minimum among the population. This best solution is denoted as  $X_{kbest,i}$ . The mean result  $M_{j,i}$  of the learners in  $j^{\text{th}}$  subject is computed. In this algorithm, the teacher always attempts to uplift the mean result of the entire class in a particular subject. Thus, the difference between the result of the teacher and mean result of the learners in each subject is represented as:

$$\text{Difference\_Mean}_{j,k,i} = r_{j,i}(X_{j,kbest,i} - T_f M_{j,i}) \quad (1)$$

where  $r_{j,i}$  is a random number between 0 and 1,  $X_{j,kbest,i}$  is the result of the best learner in  $j^{\text{th}}$  subject, and  $T_f$  is the teaching factor which chooses the value of the mean to be modified. The value of  $T_f$  can be either 1 or 2 and is decided randomly using the following equation:

$$T_f = \text{round} [1 + \text{rand} (0,1)\{2-1\}] \quad (2)$$

Based on the value of  $\text{Difference\_Mean}_{j,k,i}$ , the existing solution is upgraded using the following expression:

$$X'_{j,k,i} = X_{j,k,i} + \text{Difference\_Mean}_{j,k,i} \quad (3)$$

where  $X'_{j,k,i}$  is the updated value of  $X_{j,k,i}$ . The  $X'_{j,k,i}$  value is accepted if it has a better function value. At the end of this phase, all the accepted function values are retained which serve as the inputs to the learner phase.

#### Learner Phase

In this phase, the learners endeavor to boost their knowledge through interactions among themselves. A learner learns from other learners if they have more knowledge than him/her. For a population size of  $n$ , at  $i^{\text{th}}$  iteration, each learner is randomly compared with other learners. For this comparison, two different learners  $A$  and  $B$  are randomly chosen so that  $X'_{A,i} \neq X'_{B,i}$ , where  $X'_{A,i}$  and  $X'_{B,i}$  are the revised values at the end of the teacher phase.

$$X''_{j,A,i} = X'_{j,A,i} + r_{j,i}(X'_{j,A,i} - X'_{j,B,i}), \text{ if } f(X'_{A,i}) < f(X'_{B,i}) \quad (4)$$

$$X''_{j,A,i} = X'_{j,A,i} + r_{j,i}(X'_{j,B,i} - X'_{j,A,i}), \text{ if } f(X'_{B,i}) < f(X'_{A,i}) \quad (5)$$

If  $X''_{j,A,i}$  has a better function value, it is accepted. At  $i^{\text{th}}$  iteration, the learner phase is accomplished applying the following loops:

*Fork* = 1:*n*

Let the present learner be  $X'_{A,i}$

Randomly select another learner  $X'_{B,i}$ , so that  $X'_{A,i} \neq X'_{B,i}$

*If*  $f(X'_{A,i}) < f(X'_{B,i})$ ,

*For*  $j = 1:m$ ;  $X''_{j,A,i} = X'_{j,A,i} + r_{j,i}(X'_{j,A,i} - X'_{j,B,i})$ ; *End For*

*Else*; *For*  $j = 1:m$ ;  $X''_{j,A,i} = X'_{j,A,i} + r_{j,i}(X'_{j,B,i} - X'_{j,A,i})$ ; *End For*;

*End If*

*End For*

At the end of this phase, all the accepted function values are saved so that they become the new inputs to the teacher phase in the next generation. The flowchart for TLBO algorithm is exhibited in Fig. 1.

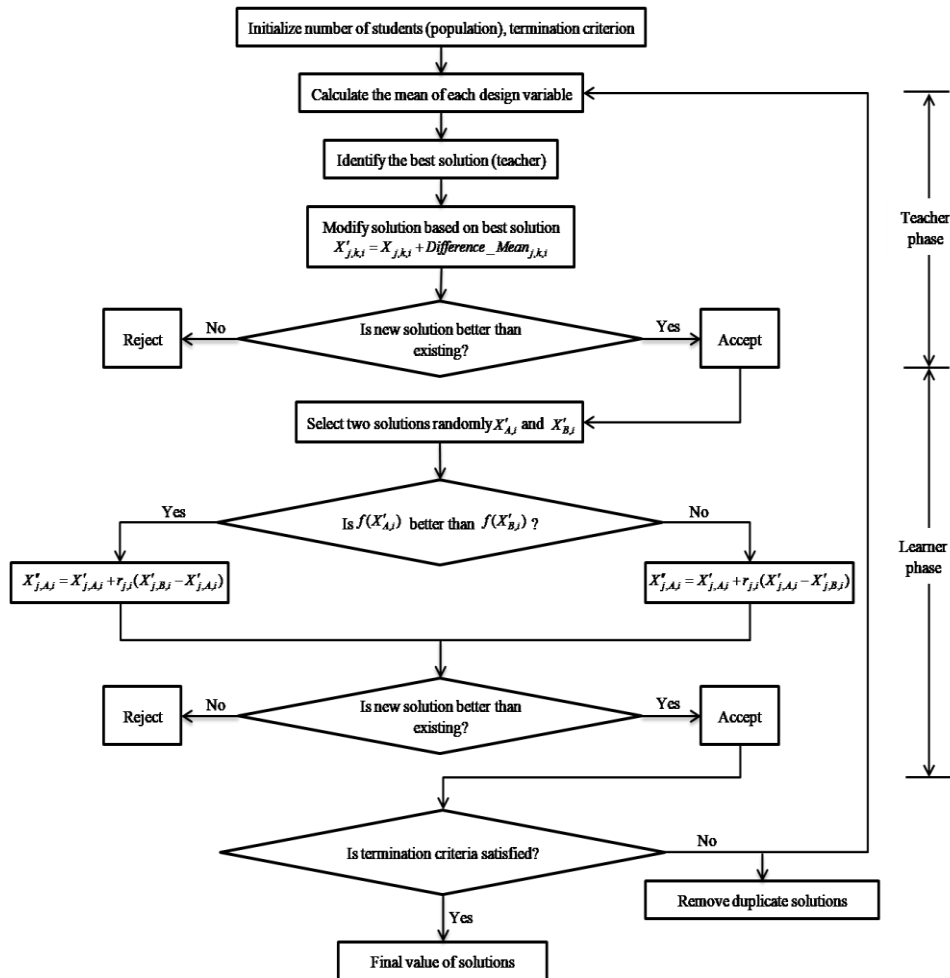


Fig. 1 Flowchart of TLBO algorithm

#### 4. EXPERIMENTAL DETAILS

This paper deals with the EDM operation for generation of standard holes on pearlitic SG iron 450/12 grade material while considering gap voltage, peak current, cycle time and rotation of the tool (electrode) as the input parameters. This work material for EDM operation is chosen due to its several favorable properties, like good wear and corrosion resistance, better castability and machinability, reasonable strength, low cost, suitability for hydraulic applications as compared to steel, malleable and grey iron castings, capability to generate intricate shapes due to better fluidity as compared to steel castings, requirement of less heat treatment resulting in better dimensional stability compared to malleable castings etc. It has found wide ranging applications in manufacturing of water pump bodies, pump housings, pump covers, pump hub for cooling system of diesel engines, manifolds for inlet

and exhaust valves, castings for engine mounting arms, engine supports, fly wheels, engine couplings, drive coupling assemblies, anti-vibration mountings, etc., pulleys for crankshaft assembly, castings for reduction gear boxes, bearing covers and end covers, castings for machine tool components, etc. The chemical composition and mechanical properties of SG iron 450/12 grade material are respectively provided in Tables 1 and 2.

**Table 1** Chemical composition of pearlitic ductile iron

Element	C	Si	Mn	P	S	Cr	Mo	Cu	Mg	Ti	Zn	Fe	Others
%	3.365	2.393	0.238	0.072	<0.150	0.007	<0.010	0.37	0.085	0.032	0.027	90.75	2.661

**Table 2** Mechanical properties of pearlitic SG iron (450/12 grade)

Mechanical property	Value
Tensile strength	450 MPa
Yield strength	310 MPa
Elongation	12%
Hardness	197 BHN
Density	6.95 gm/cm <sup>3</sup>
Relative wear resistance	Excellent

**Table 3** EDM process parameters with their operating levels

Process parameter	Symbol	Unit	Level				
			-2	-1	0	1	2
Gap voltage	$x_1$	V	40	45	50	55	60
Peak current	$x_2$	A	20	30	40	50	60
Cycle time	$x_3$	$\mu$ s	80	160	240	320	400
Tool rotation	$x_4$	rpm	5	15	25	35	45

While performing EDM operation on pearlitic SG iron 450/12 grade material, each of the considered EDM process parameters has been varied at five different operating levels, as shown in Table 3. According to the central composite design plan, for four factors with five levels, 30 experiments have been conducted in an Agietron 250 C EDM set-up. It has the following specifications, e.g. working area: [X 700 Y 500 Z 500] mm, maximum workpiece dimension: [L 1000 W 700 H 320] mm, maximum workpiece weight: 1200 kg, maximum electrode weight: 400 kg, work tank volume: 360 l, dielectric unit capacity: 1200 l and accuracy: 0.001 mm. The photograph of the EDM set-up is shown in Fig. 2. During the machining operation, Castrol SE 180 EDM fluid is used as the dielectric because of its various advantageous properties, like low odor, higher stability with extended fluid life, low viscosity, high flash point, increased reliability and safe use. The specimen size has been taken as 15 × 40 mm.

**Table 4** Details of experimental results

Exp. No.	Gap voltage	Peak current	Cycle time	Rotation	MRR	SR	TWR	OC	CE
1	50	20	240	25	6.00	8.572	0.589	0.8084	0.2914
2	40	40	240	25	16.60	8.581	0.671	0.8495	0.2982
3	50	40	240	45	13.07	8.092	0.623	0.8473	0.1495
4	50	60	240	25	21.07	8.532	0.698	0.8606	0.3055
5	50	40	240	25	11.98	8.712	0.612	0.8333	0.3012
6	50	40	240	5	9.28	9.612	0.599	0.8295	0.3197
7	60	40	240	25	15.98	8.902	0.663	0.8493	0.2998
8	50	40	400	25	23.26	8.742	0.726	0.9266	0.3032
9	50	40	80	25	4.10	8.622	0.531	0.7623	0.2989
10	50	40	240	25	15.21	8.531	0.659	0.8492	0.3011
11	45	30	320	35	7.41	8.235	0.590	0.8077	0.1932
12	55	30	320	15	6.10	9.092	0.586	0.8095	0.3176
13	50	40	240	25	13.07	8.626	0.627	0.8446	0.3014
14	45	30	160	15	2.25	9.207	0.522	0.7233	0.3143
15	55	50	320	15	18.14	9.367	0.677	0.8543	0.3179
16	45	30	160	35	2.16	8.265	0.518	0.7154	0.1795
17	45	50	320	15	19.29	9.247	0.696	0.8559	0.3174
18	45	50	160	35	4.98	8.635	0.545	0.7827	0.1934
19	50	40	240	25	9.95	8.732	0.597	0.8297	0.3019
20	55	30	160	35	3.59	8.475	0.529	0.7345	0.2236
21	55	30	160	15	1.97	9.212	0.511	0.7154	0.3161
22	55	50	160	35	6.25	8.685	0.593	0.8246	0.2579
23	55	30	320	35	22.13	8.345	0.719	0.9118	0.2003
24	50	40	240	25	12.84	8.826	0.618	0.8393	0.3015
25	45	50	320	35	19.78	8.436	0.692	0.8604	0.2693
26	45	50	160	15	4.96	9.232	0.548	0.7725	0.3156
27	55	50	320	35	21.24	8.176	0.702	0.8988	0.2009
28	50	40	240	25	11.06	8.696	0.605	0.8306	0.3018
29	55	50	160	15	5.65	9.172	0.552	0.7935	0.3164
30	45	30	320	15	5.80	9.497	0.567	0.8077	0.3183

It is worthwhile to mention here that all the 30 experiment runs have been performed in random order so that the machining error can be minimized. Five most important responses (outputs) of the EDM process are considered here, i.e. MRR (in mm<sup>3</sup>/min), SR (in  $\mu$ m), EWR (in mm<sup>3</sup>/min), OC (in mm) and CE (in mm). For measurement of MRR and EWR, an electronic weighing balance (A&D GR-202 type) has been employed. On the other hand, SR has been measured using HommelWerke Turbo Wave V7.20 roughness tester, and ZEISS O-INSPECT 442 CMM machine (with GEOMET universal CMM software) has been used for measuring both OC and CE. Table 4 displays the experimental design plan along with the measured values of the considered responses. In Fig. 3, the photographs of the copper electrode utilized during EDM operation and the machined component are provided. Among these responses, MRR is the sole larger-the-better quality characteristic, and the remaining three are of smaller-the-better type.



**Fig. 2** EDM set-up



**Fig. 3** Round copper tool and machined component (5 mm depth and 20 mm dia.)

### 5. OPTIMIZATION OF THE EDM PROCESS

Now, based on the experimental data of Table 4 and using Minitab software (R17), the following RSM-based equations are developed for the five responses, considering the main, second order and interaction effects between the considered EDM process parameters. Higher values of the corresponding coefficient of determination ( $R^2$ ) justify that these RSM-based equations are the best fit models depicting the relationships between the process parameters and responses.

$$Y(MRR) = -5.0 + 0.235x_1 + 0.727x_2 - 0.05x_3 - 1.436x_4 - 0.0174x_1x_2 + \dots \\ 0.0241x_1x_4 + 0.00196x_2x_3 + 0.00149x_3x_4 \quad (R^2 = 81.57) \quad (6)$$

$$Y(SR) = 9.57433 + 0.00305x_1 + 0.00207x_2 - 0.000105x_3 - 0.0407x_4 \quad (R^2 = 85.47) \quad (7)$$

$$Y(TWR) = 0.54 - 0.0134x_1 + 0.0073x_2 + 0.000319x_3 + 0.00329x_4 + \dots \\ 0.000201x_1^2 - 0.000008x_2^2 - 0.000001x_3^2 - 0.00009x_4^2 - \dots \\ 0.00013x_1x_2 + 0.000011x_2x_4 + 0.00001x_3x_4 \quad (R^2 = 84.59) \quad (8)$$

$$Y(OC) = 0.147 + 0.0101x_1 + 0.01212x_2 + 0.01184x_3 - 0.00912x_4 - 0.000133x_1^2 - \dots \\ 0.000071x_2^2 - 0.0000001x_3^2 - 0.000061x_4^2 - 0.000022x_1x_2 + 0.000238x_1x_4 - \dots \\ 0.000012x_2x_3 - 0.000014x_2x_4 + 0.000008x_3x_4 \quad (R^2 = 84.59) \quad (9)$$

$$Y(CE) = -0.162 + 0.016x_1 + 0.00459x_2 + 0.000158x_3 - 0.00091x_4 - \dots \\ 0.000142x_1^2 - 0.000037x_2^2 - 0.000196x_4^2 - 0.000069x_1x_2 + 0.000056x_1x_4 + \dots \quad (10) \\ 0.000002x_2x_3 + 0.000077x_2x_4 \quad (R^2 = 90.56)$$

**Table 5** Results of single-objective optimization

Response	Method	Mean	SD	Optimal value	Parameter			
					Gap voltage	Peak current	Cycle time	Tool rotation
MRR	FA	40.629	1.169	40.824	60	55.172	387.421	45
	DE	38.952	0.576	39.022	55.03	58.75	393.49	39.363
	CS	41.316	1.201	41.508	56.457	57.999	392.36	44.76
	TLBO	44.629	0.246	44.660	60	60	400	45
SR	FA	7.938	0.001	7.904	43.482	32.00	361.18	45
	DE	8.009	0.001	7.987	58.05	27.39	194.14	44.23
	CS	8.01	0.017	7.883	40	27.85	372.16	45
	TLBO	7.874	0.0009	7.864	40	20	400	45
TWR	FA	0.481	0.004	0.480	50.5481	42.169	110.778	45
	DE	0.435	0.01	0.434	45.975	26.991	93.612	45
	CS	0.437	0.009	0.436	46.963	30.184	88.668	45
	TLBO	0.403	0.00069	0.402	40.024	20.001	80	45
OC	FA	0.689	0.005	0.688	45.813	23.817	173.132	43.464
	DE	0.626	0.008	0.625	43.351	26.565	117.224	44.966
	CS	0.605	0.006	0.604	43.014	28.959	86.787	45
	TLBO	0.515	0.002	0.514	40.024	20.215	80	45
CE	FA	0.078	0.002	0.077	45.77	26.02	116.07	45
	DE	0.058	0.004	0.057	45.86	20.05	94.71	44.68
	CS	0.060	0.004	0.059	43.66	25.411	81.892	45
	TLBO	0.021	0.001	0.020	40	20	80	45

It has already been mentioned that this paper focuses on the applications of four popular metaheuristic algorithms in the form of FA, DE, CS and TLBO techniques for both single- and multi-objective optimization of the considered EDM process. While solving this parametric optimization problem using the considered algorithms, the corresponding values of different algorithmic parameters are set as follows:

FA: Number of iterations = 500, number of fireflies = 300, light absorption coefficient = 1, initial randomness = 0.9, randomness factor = 0.91 and randomness reduction = 0.75.

DE algorithm: Number of iterations = 500, population size = 300, lower bound of scaling factor = 0.2, upper bound of scaling factor = 0.8 and crossover probability = 0.9.

CS algorithm: Number of iterations = 500, population size (nests) = 300 and discovering rate of alien eggs = 0.25.

TLBO algorithm: Number of iterations = 500 and population size = 300.

For single objective optimization, the developed equations are solved using the considered metaheuristics within the given sets of constraints as  $40 \leq x_1 \leq 60$ ,  $20 \leq x_2 \leq 60$ ,  $80 \leq x_3 \leq 400$  and  $5 \leq x_4 \leq 45$ . The results of this single objective optimization are provided in Table 5. It can be clearly unveiled from the table that among the four metaheuristics, the TLBO algorithm has the superiority over the others with respect to better values of the responses with higher accuracy and lower standard deviation (SD). The results of single objective optimization derive the optimal settings of the four EDM process parameters to be

maintained for maximization/minimization of the considered responses. The boxplots of Fig. 4 prove that the optimal solutions derived using the TLBO algorithm are more consistent having the lowest variability as compared to others. On the other hand, the convergence diagrams, as exhibited in Fig. 5, also demonstrate that TLBO algorithm requires less computational effort with respect to both computation speed and time. It can be interestingly noticed that the TLBO algorithm provides the optimal solutions for all the five EDM responses almost within 5-10 iterations.

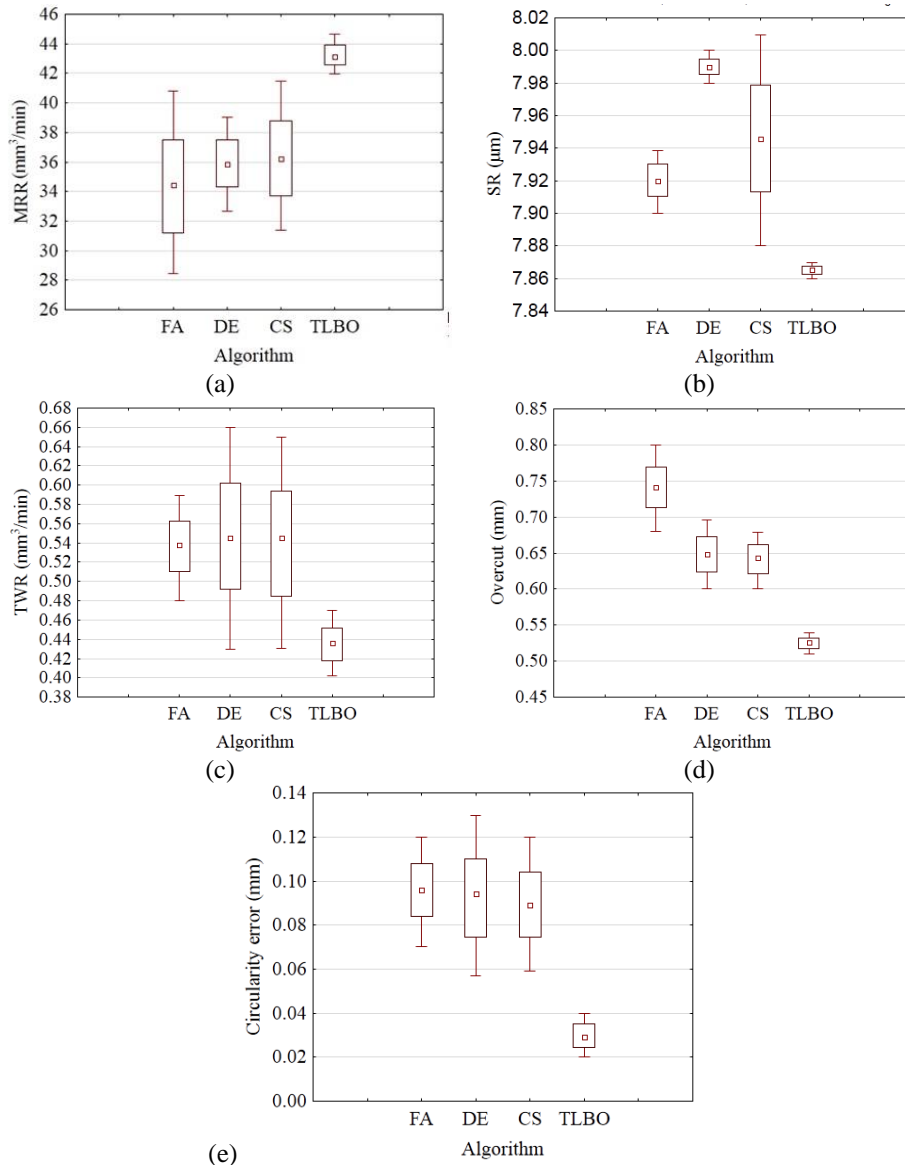


**Fig. 4** Boxplots for the considered metaheuristic algorithms

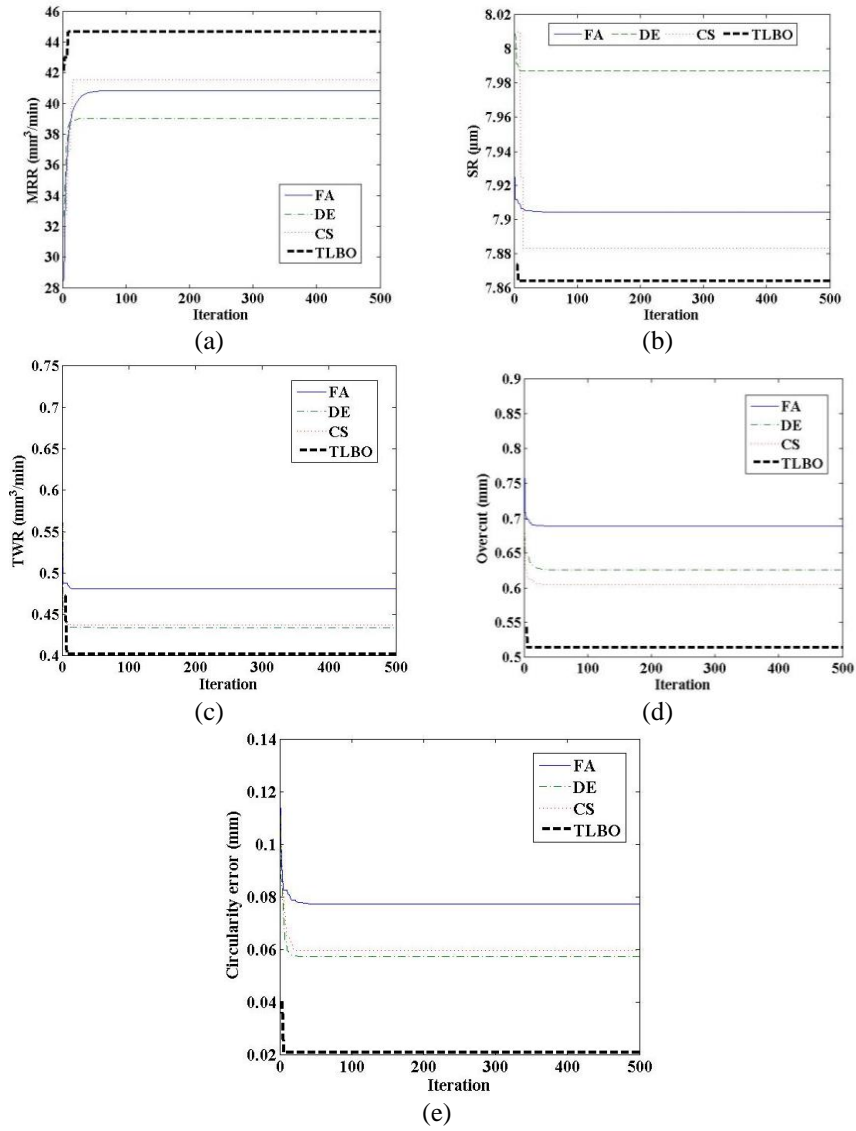


**Fig. 5** Convergence diagrams for the metaheuristic algorithms

**Table 6** *t*-test results with respect to the TLBO algorithm

Response	FA	DE	CS
MRR	74.817	204.362	60.383
SR	-272.183	-1423.66	-28.1014
TWR	-205.229	-57.451	-63.872
OC	-627.432	-351.727	-436.548
CE	-409.364	-183.558	-191.048

Finally, in order to validate the uniqueness of the TLBO algorithm over the remaining three optimization techniques, two-tailed paired  $t$ -tests are performed with the null hypothesis and alternative hypothesis as  $H_0(\mu_A = \mu_B)$  and  $H_a(\mu_A \neq \mu_B)$  respectively (where  $\alpha$  is the level of significance, and  $\mu_A$  and  $\mu_B$  are respectively the mean response values obtained using two algorithms being pair-wise compared). The results of the paired  $t$ -tests are provided in Table 6. In this table, as the absolute values of  $t$ -statistic for all the responses for the pair-wise comparisons between TLBO and other algorithms are greater than the corresponding tabulated  $t$ -value, the null hypotheses can be rejected. It thus demonstrates the uniqueness of the optimization performance of the TLBO algorithm against the other techniques while providing the best single objective optimization solutions.

Based on the optimal solutions provided by the TLBO algorithm, effects of the EDM process parameters under consideration on the responses are investigated using the developed response graphs of Figs. 6-10. Fig. 6 exhibits how the obtained MRR changes with varying values of the process parameters. It can be interestingly noticed that with the increasing values of all the EDM process parameters, the MRR values also increase. Higher values of gap voltage, peak current and cycle time cause the available discharge energy to increase, resulting in more melting and vaporization of material from the workpiece. The impulsive force in the spark gap also increases, which is responsible for higher MRR [25].

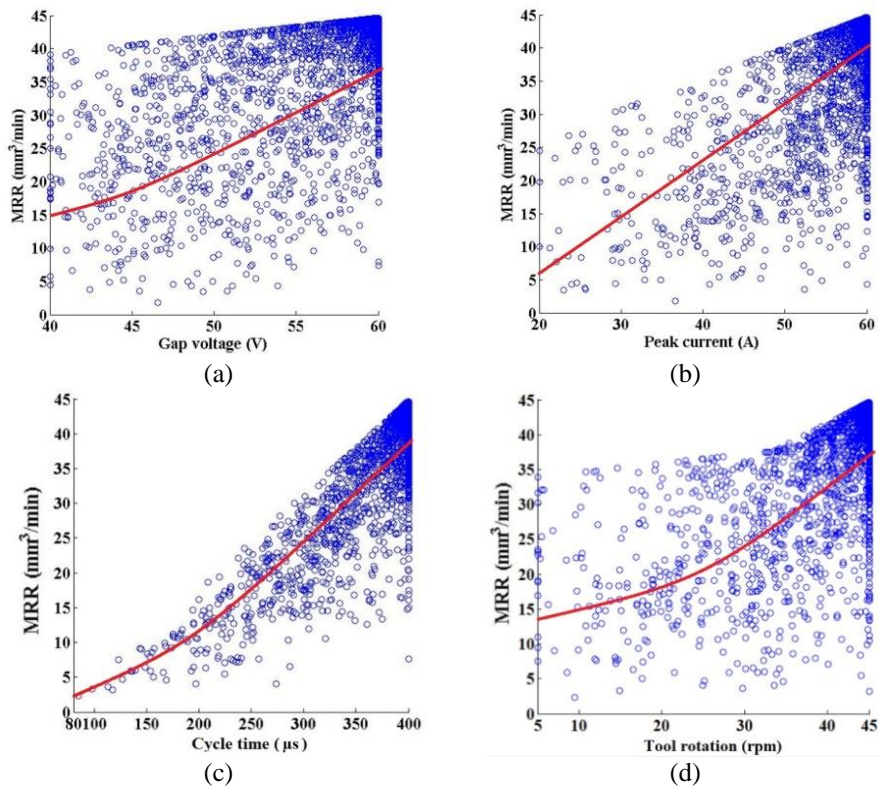


**Fig. 6** Effects of EDM process parameters on MRR

In this EDM process, the tool (electrode) rotates normal to the workpiece surface and a centrifugal force is thus generated causing more debris removal from the machining zone. Tool rotation in the EDM process also results in formation of a thin recast layer, and the debris get easily cleared from the melt pool while exposing the workpiece to increased spark intensity. Thus, less material remains in the melt cavity to be re-deposited over the workpiece surface [26]. Tool rotation eases the flushing problem as encountered during the EDM operation.

The influences of the EDM process parameters on the SR are exhibited in Fig. 7. With increasing values of gap voltage and peak current, the SR of the machined components slightly increases. It almost remains unaffected due to the changes in cycle time and it shows a decreasing trend pattern with increasing values of tool rotation. The increments in gap voltage, peak current and cycle time are responsible for stronger discharge energy, creating higher temperature and formation of larger craters on the machined surface, resulting in poor surface quality [27]. It is also noticed that the tool rotation helps in a quick removal of the debris from the machining zone and as a result, with a higher tool rotation, the machined surface becomes smoother. With the tool rotation, it is expected that there would be 9-10% decrease in the average SR value.

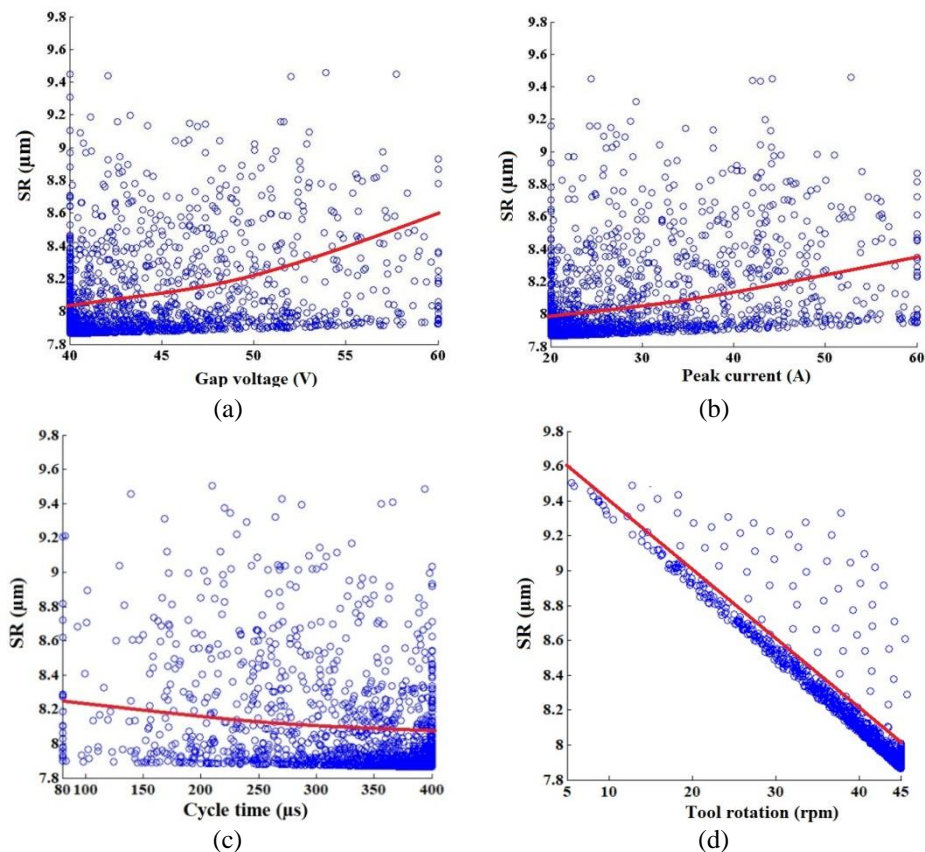


**Fig. 7** Effects of the EDM process parameters on the SR

As revealed from Fig. 8, higher values of gap voltage, peak current and cycle time cause increments in the TWR values. At those higher parametric settings, there are micro tool wears due to availability of higher spark energy density at the machining zone. Generally, lower settings of these three EDM process parameters tend to enhance the possibility of carbon deposition on the tool surface, which finally helps in lowering the value of the TWR. On the contrary, with increment in tool rotational speed, there is also a possibility of throwing away the carbon particles from the tool surface, which causes an increment in the TWR. But, at higher tool rotation, better flushing occurs and there is a better disposition of dielectric fluid in the machining zone, leading to smaller TWR [28].

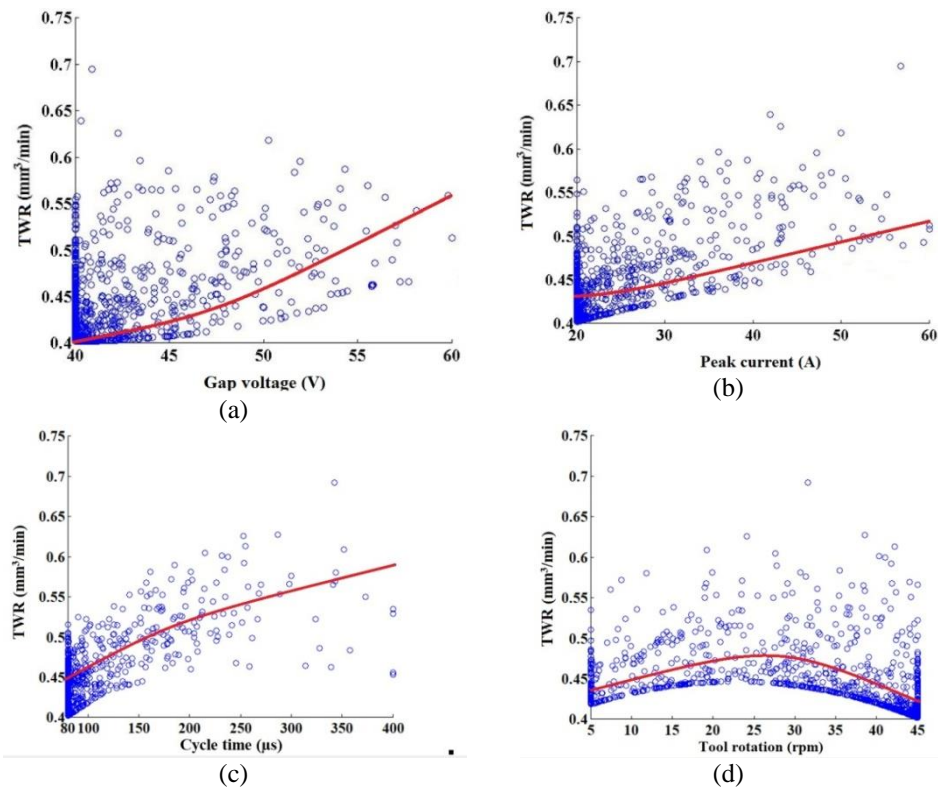


**Fig. 8** Effects of the EDM process parameters on the TWR

During the EDM operation, OC occurs due to side erosion and removal of debris. It shows increasing trend patterns with increased values of gap voltage, peak current and cycle time, as exhibited in Fig. 9. At higher settings of these three EDM process parameters, availability of higher gap voltage and gap width allows breakdown of dielectric at a wide gap due to higher electric field [29, 30]. At higher gap voltage and peak current, spark energy density would be more with faster machining rate, which is also responsible for higher OC. But, with increasing tool rotational speed, OC gradually increases. Increased centrifugal force, resulting from a higher tool rotation, removes more debris from the machining zone. The removed debris is placed between the side wall of the electrode and

workpiece, causing generation of a spark between them. It leads to higher OC. At a higher tool rotational speed, there would be more turbulence taking place at the machining zone which would perhaps be responsible for removal of the debris, leading to gradual decrement in OC.

The CE in the machined components occurs due to non-uniform undercut and overcut which can be effectively controlled by proper settings of different EDM process parameters. As noticed in Fig. 10, with increasing values of gap voltage, peak current and cycle time, CE shows an increasing trend pattern. It is also affected by tool rotation. At a higher gap voltage, peak current and cycle time, there are occurrences of secondary spark discharges caused by poor flushing, which are responsible for inferior CE. Increase in CE is also occurred due to high tool wear and sporadic machining at higher voltage [31]. A higher tool rotational speed may create turbulence of the dielectric fluid at the machining zone, which would be responsible for removal of debris from the external periphery of the machined hole. Thus, there may be a high chance of obtaining lower CE at higher tool rotation.

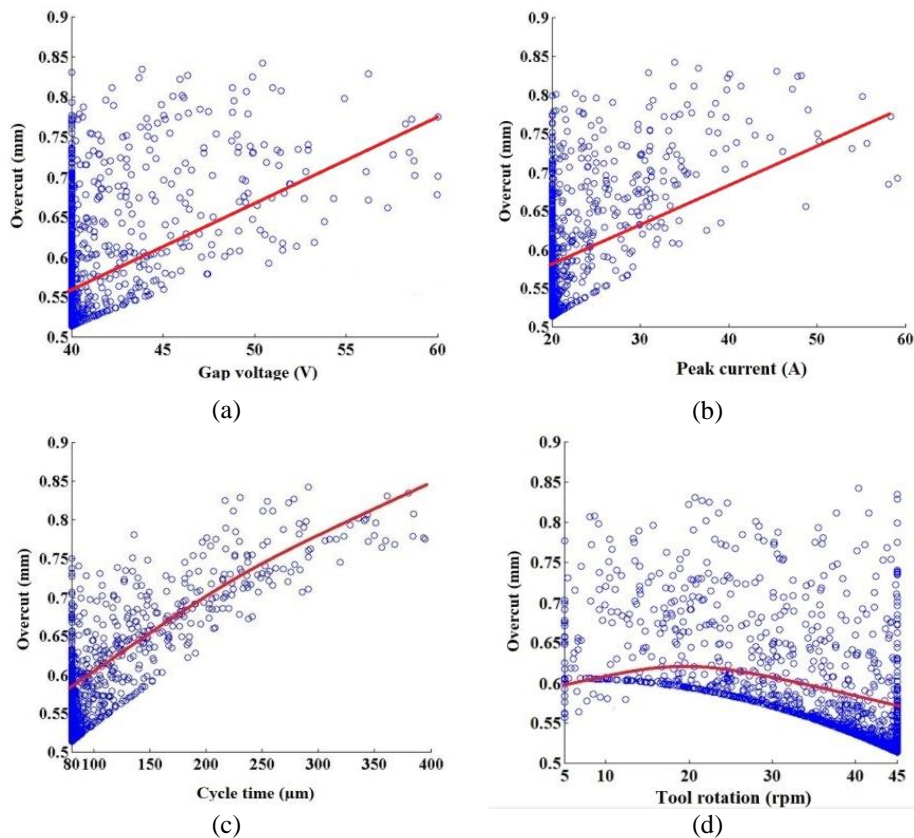


**Fig. 9** Effects of the EDM process parameters on the OC

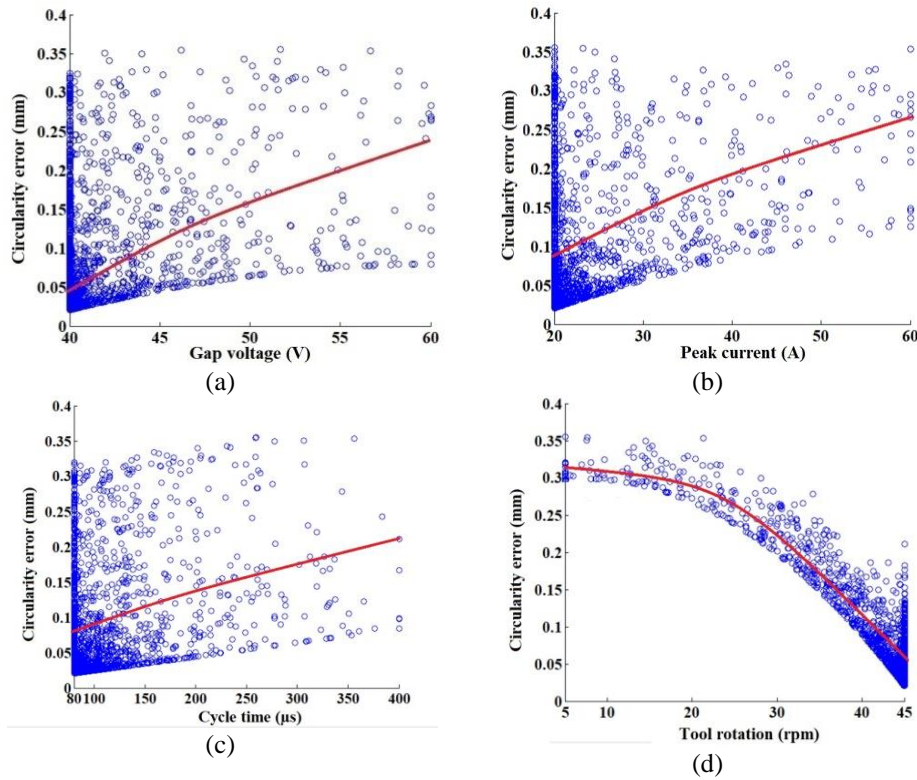


**Fig. 10** Effects of the EDM process parameters on the CE

It can be noticed from the results of single objective optimization of the considered EDM process that separate parametric settings are obtained for different responses based on the applications of four metaheuristic algorithms. But, in a real time machining environment, it is never possible for an operator to set the EDM process parameters at different operating levels in a single EDM set-up. It is thus always advised to derive a unique combination of the process parameters so as to simultaneously optimize all the five responses. For this purpose, the following multi-objective optimization model is developed which is subsequently solved using the considered metaheuristics.

$$\text{Minimize } Z = -\frac{w_1 Y(\text{MRR})}{(\text{MRR})_{\max}} + \frac{w_2 Y(\text{SR})}{(\text{SR})_{\min}} + \frac{w_3 Y(\text{EWR})}{(\text{EWR})_{\min}} + \frac{w_4 Y(\text{OC})}{(\text{OC})_{\min}} + \frac{w_5 Y(\text{CE})}{(\text{CE})_{\min}} \quad (11)$$

where  $w_1$ ,  $w_2$ ,  $w_3$ ,  $w_4$  and  $w_5$  are the weights allotted to MRR, SR, EWR, OC and CE respectively,  $(\text{MRR})_{\max}$  is the maximum value of MRR,  $(\text{SR})_{\min}$ ,  $(\text{EWR})_{\min}$ ,  $(\text{OC})_{\min}$  and  $(\text{CE})_{\min}$  are the minimum values of SR, EWR, OC and CE, respectively. These values are obtained from the results of single objective optimization of the responses. In this paper, equal weights are assigned to all the responses under consideration. The solutions of this multi-objective optimization problem are provided in Table 7. It can be clearly unveiled from this table that the TLBO algorithm again excels over the remaining three metaheuristics with

respect to accuracy and consistency of the derived optimal solutions. Thus, for obtaining the most desired performance of the EDM process while generating standard holes on pearlitic SG iron 450/12 grade work material, it is always recommended to set the input parameters as gap voltage = 41 V, peak current = 58.58 A, cycle time = 285  $\mu$ s and tool rotation = 45 rpm. Thus, based on the optimal solutions derived using TLBO algorithm, it can be concluded that lower gap voltage, higher peak current, moderate cycle time and higher tool rotational speed would concurrently optimize all the responses of the considered EDM process.

Table 8 exhibits the percentage improvements in the response values based on the multi-objective optimization results of the TLBO algorithm against FA, DE and CS techniques. It can be observed from this table that for the considered EDM process, the values of MRR, SR, TWR, OC and CE are significantly improved employing the TLBO algorithm as compared to other metaheuristic algorithms.

**Table 7** Results of multi-objective optimization

Method	Response	Mean	SD	Optimal value	Z	Parameter			
						Gap voltage	Peak current	Cycle time	Tool rotation
FA	MRR	2.229	0.107	23.2	2.225	43.258	56.25	290	45
	SR			7.96					
	TWR			0.436					
	OC			0.8					
	CE			0.182					
DE	MRR	2.309	0.152	21.953	2.303	42.3	57.25	278.35	45
	SR			7.961					
	TWR			0.428					
	OC			0.788					
	CE			0.181					
CS	MRR	2.293	0.192	22.808	2.284	41.23	58.23	283.56	45
	SR			7.959					
	TWR			0.434					
	OC			0.779					
	CE			0.179					
TLBO	MRR	2.223	0.09	24.012	2.218	41	58.58	285	45
	SR			7.959					
	TWR			0.409					
	OC			0.708					
	CE			0.178					

**Table 8** Percentage improvements in responses using the TLBO algorithm

Response	FA	DE	CS
MRR	3.5	9.37	5.27
SR	0.75	0.75	0
TWR	6.19	4.43	5.76
OC	11.5	10.15	9.11
CE	2.19	1.65	0.55

## 6. CONCLUSIONS

The paper studies the capability of an EDM process in generating standard holes on pearlitic SG iron 450/12 grade material, which has found wide ranging applications in manufacturing of diverse mechanical components. The optimal settings of gap voltage, peak current, cycle time and tool rotation for the considered machining application are determined using the TLBO algorithm. It is observed that lower gap voltage, higher peak current, moderate cycle time and higher tool rotational speed would simultaneously optimize material removal rate, surface roughness, tool wear rate, radial overcut and circularity error of this EDM process. The effects of all these EDM process parameters on the responses are also investigated. The optimization performance of the TLBO algorithm is compared with three other metaheuristics, and it is concluded that the TLBO algorithm excels over the others with respect to higher accuracy of the optimal solutions with low variability and less computational effort. The results of the paired *t*-tests and developed boxplots also confirm this observation. This algorithm provides almost global optimal solutions for both single- and multi-objective optimization problems as it is least affected due the settings of its different tuning parameters. The applicability of this algorithm for optimization of other conventional and non-conventional machining processes can also be explored. The effects of changing weights allotted to different responses on the optimization performance of TLBO algorithm can be examined as the future scope of this paper.

## REFERENCES

1. El-Hofy, H., 2005, *Advanced Machining Processes: Nontraditional and Hybrid Machining Processes*, McGraw-Hill, New York, USA.
2. Pandey, P.C., Shan, H.S., 2005, *Modern Machining Processes*, Tata MacGraw-Hill Publishing Com. Ltd., New Delhi, India.
3. Qudeiri, J.E.A., Mourad, A-H.I., Ziout, A., Abidi, M.H., Elkaseer, A., 2018, *Electric discharge machining of titanium and its alloys: Review*, International Journal of Advanced Manufacturing Technology, 96(1-4), pp. 1319-1339.
4. Gangil, M., Pradhan, M.K., Purohit, R., 2017, *Review on modelling and optimization of electrical discharge machining process using modern techniques*, Materials Today: Proceedings, 4(2), pp. 2048-2057.
5. Mandal, D., Pal, S.K., Saha, P., 2007, *Modeling of electrical discharge machining process using backpropagation neural network and multi-objective optimization using non-dominating sorting genetic algorithm-II*, Journal of Materials Processing Technology, 186(1-3), pp. 154-162.
6. Bharti, P.S., Maheshwari, S., Sharma, C., 2012, *Multi-objective optimization of electric-discharge machining process using controlled elitist NSGA-II*, Journal of Mechanical Science and Technology, 26(6), pp. 1875-1883.
7. Baraskar, S.S., Banwait, S.S., Laroia, S.C., 2013, *Multiobjective optimization of electrical discharge machining process using a hybrid method*, Materials and Manufacturing Processes, 28(4), pp. 348-354.
8. Shivakoti, I., Kibria, G., Diyaley, S., Pradhan, B.B., 2013, *Multi-objective optimization and analysis of electrical discharge machining process during micro-hole machining of D3 die steel employing salt mixed de-ionized water dielectric*, Journal of Computational and Applied Research in Mechanical Engineering, 3(1), pp. 27-39.
9. Aich, U., Banerjee, S., 2014, *A simple procedure for searching Pareto optimal front in machining process: Electric discharge machining*, Modelling and Simulation in Engineering Article ID 594054: 12 pages, <http://dx.doi.org/10.1155/2014/594054>.
10. Radhika, N., Shivaram, P., Vijay Karthik, K.T., 2014, *Multi-objective optimization in electric discharge machining of aluminium composite*, Tribology in Industry, 36(4), pp. 428-436.
11. Tiwari, R.K., 2015, *Multi-objective optimization of electrical discharge machining process parameters using genetic algorithm*, International Journal of Engineering Research and General Science, 3(3), pp. 1411-1423.

12. Mazarbhuiya, R.M., Choudhury, P.K., Rahang, M., 2016, *Taguchi-grey relational based multi-objective optimization of process parameters in electric discharge machining of aluminium with copper electrode*, Journal of Basic and Applied Engineering Research, 3(13), pp. 1169-1171.
13. Mohanty, C.P., Mahapatra, S.S., Singh, M.R., 2016, *A particle swarm approach for multi-objective optimization of electrical discharge machining process*, Journal of Intelligent Manufacturing, 27(6), pp. 1171-1190.
14. Gohil, V., Puri, Y.M., 2017, *Multi-objective optimization of material removal rate and surface roughness in electrical discharge turning of titanium alloy (Ti-6Al-V)*, Indian Journal of Engineering & Materials Sciences, 24(6), pp. 429-436.
15. Satpathy, A., Tripathy, S., Senapati, N.P., Brahma, M.K., 2017, *Optimization of EDM process parameters for AlSiC-20% SiC reinforced metal matrix composite with multi response using TOPSIS*, Materials Today: Proceedings, 4, pp. 3043-3052.
16. Mohanty, U.K., Rana, J., Sharma, A., 2017, *Multi-objective optimization of electro-discharge machining (EDM) parameter for sustainable machining*, Materials Today: Proceedings, 4(2), pp. 9147-9157.
17. Singh, B., Kumar, S., Kumar, J., 2017, *Multi-objective optimization in electrical discharge machining of 6061 Al/SiCp using RSM and NSGA-II*, Key Engineering Materials, 748, pp. 207-211.
18. Gostimirovic, M., Pucovsky, V., Sekulic, M., Radovanovic, M., Madic, M., 2018, *Evolutionary multi-objective optimization of energy efficiency in electrical discharge machining*, Journal of Mechanical Science and Technology, 32(10), pp. 4775-4785.
19. Ramprabhu, T., Savsani, V., Parsana, S., Radadia, N., Sheth, M., Sheth, N., 2018, *Multi-objective optimization of EDM process parameters by using passing vehicle search (PVS) algorithm*, Defect and Diffusion Forum, 382, pp. 138-146.
20. Tharian, B.K., Jacob, E., Johnson, J., Hari, V., 2019, *Multi-objective parametric optimization in EDM using grey relational analysis*, Materials Today: Proceedings, 16(2), pp. 1013-1019.
21. Huu, P.N., Tien, L.B., Duc, Q.T., Van, D.P., Xuan, C.N., Van, T.N., Duc, L.N., Jamil, M., Khan, A.M., 2019, *Multi-objective optimization of process parameter in EDM using low-frequency vibration of workpiece assigned for SKD61*, Sadhana, 44, 211, <https://doi.org/10.1007/s12046-019-1185-y>.
22. Niamat, M., Sarfraz, S., Ahmad, W., Shehab, E., Saloniitis, K., 2020, *Parametric modelling and multi-objective optimization of electro discharge machining process parameters for sustainable production*, Energies, 13(1), 20 pages, doi:10.3390/en13010038.
23. Rao, R.V., Savsani, V.J., Vakharia, D.P., 2011, *Teaching-learning-based optimization: a novel method for constrained mechanical design optimization problems*, Computer-Aided Design, 43(3), pp. 303-315.
24. Diyaley, S., Chakraborty, S., 2019, *Optimization of multi-pass face milling parameters using metaheuristic algorithms*, FactaUniversitatis-Series Mechanical Engineering, 17(3), pp. 365-383.
25. Gopalakannan, S., Senthivelan, T., Ranganathan, 2012, *Modeling and optimization of EDM process parameters on machining of Al7075-B<sub>4</sub>C MMC using RSM*, Procedia Engineering, 38, pp. 685-690.
26. Dwivedi, A.P., Choudhury, S.K., 2016, *Effect of tool rotation on MRR, TWR, and surface integrity of AISI-D3 steel using the rotary EDM process*, Materials and Manufacturing Processes, 31(14), pp. 1844-1852.
27. Kiyak, M., Çakır, O., 2007, *Examination of machining parameters on surface roughness in EDM of tool steel*, Journal of Materials Processing Technology, 191(1-3), pp. 141-144.
28. Lin, Y.C., Lee, H.S., 2008, *Machining characteristics of magnetic force-assisted EDM*, International Journal of Machine Tools and Manufacture, 48(11), pp. 1179-1186.
29. Pradhan, B.B., Masanata, M., Sarkar, B.R., Bhattacharyya, B.B., 2009, *Investigation of electro-discharge micro-machining of titanium super alloy*, International Journal of Advanced Manufacturing Technology, 41, pp. 1094-1106.
30. Jahan, M.P., Wong, Y.S., Rahman, M., 2008, *A study on the fine-finish die-sinking micro-EDM of tungsten carbide using different electrode materials*, Journal of Materials Processing Technology, 209(8), pp. 3956-3967.
31. Alshemary, A., Pramanik, A., Basak, A.K., Littlefair, G., 2018, *Accuracy of duplex stainless steel feature generated by electrical discharge machining (EDM)*, Measurement, 130, pp. 137-144.